CSIAM Trans. Life Sci.
doi: 10.4208/csiam-ls.SO-2025-0017

Vol. **2**, No. 1, pp. 133-153
March 2026

Mathematical Modeling of Green Sea Turtle Population Dynamics Under Environmental and Thermal Constraints

Baojun Song*

School of Computing, Montclair State University, Montclair, NJ 07043, USA.

Received 31 May 2025; Accepted 23 October 2025

This work is dedicated to Professor Zhien Ma, who led me into the realm of mathematical biology, in honor of his 90th birthday.

Abstract. Global warming and deteriorating environmental conditions have raised concerns about the persistence of green sea turtle populations, whose reproduction is governed by temperature-dependent sex determination. This study employs mathematical modeling to investigate these ecological challenges. Building on our previous models of green sea turtle population dynamics, we develop a sex-structured and stage-structured life history model that integrates temperature-dependent sex determination and ecological viability, offering a mechanistic framework for understanding green sea turtle population dynamics under climate and environmental stress. Our findings reveal that population dynamics are governed by an Allee-adjusted reproductive number, which accounts for both thermal and environmental influences. Additionally, we conduct a global stability analysis of the collapsed equilibrium using the singular perturbation approach, offering insights into long-term population viability. While additional parameter validation is necessary for definitive conclusions, our results illustrate how climate change and deteriorating environmental conditions shape the long-term viability of green sea turtle populations.

AMS subject classifications: 37G10, 92-10 , 92D25, 92D40

Key words: Temperature-dependent sex determination, green sea turtle, sex-structured and stage-structured, Allee effects, population collapse, bi-stability.

1 Introduction

Green sea turtles (Chelonia mydas) are long-lived marine reptiles, with lifespans exceeding 70 years [5, 15, 26, 32]. As depicted in Fig. 1, their life cycle consists of four distinct stages: egg, hatchling, juvenile, and adult.

*Corresponding author. *Email address:* songb@mail.montclair.edu (B. Song)

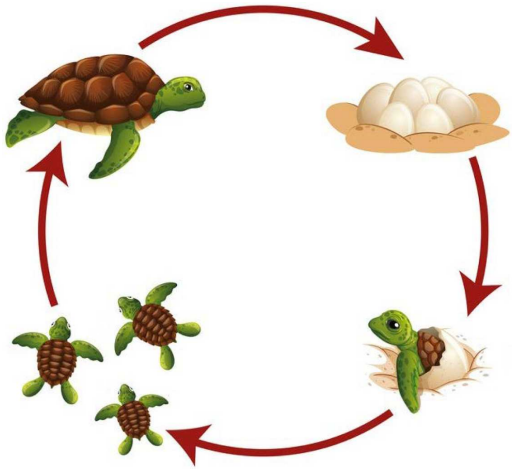

Figure 1: Life cycle of green sea turtles, comprising four stages: egg, hatchling, juvenile, and adult.

They begin as eggs laid on nesting beaches, incubate in the sand, and hatch into small hatchlings that immediately move toward the ocean. As juveniles, they develop in nearshore waters before reaching sexual maturity, often requiring several years or even decades. Adult green turtles, particularly females, make long migrations to nesting beaches to lay eggs, repeating this cycle every few years [32].

The incubation period lasts approximately 45 to 70 days, during which the mean nest temperature determines the sex of the hatchlings, a phenomenon known as temperature-dependent sex determination (TSD). This discovery dates back to Charnier's seminal work [9] in 1966 at the University of Dakar, Senegal. Before then, sex determination in vertebrates was assumed to be strictly genetically controlled. During the past half century, extensive research has expanded this understanding to reptiles.

Comprehensive reviews of TSD include Bull's pioneering work [7], Valenzuela and Lance's field review [38], the introductory book by Lutz *et al.* [24] and Hall's open-access publication [17].

TSD is a process in which environmental temperature influences embryonic development by triggering the production of sex hormones, thus dictating the sex of the embryo. This mechanism, categorized as the determination of environmental sex, is based on physical and biotic factors such as temperature [27, 29]. Every reptile species that exhibits TSD has a thermosensitive period, during which sex differentiation occurs. In turtles, this critical period occurs mid-trimester of the incubation cycle [3].

While many reptile species rely on genetically determined sex via zygotic sex chromosome composition, others – including crocodilians, most turtles, and some lizards – determine sex through incubation temperature during early gonadal differentiation. TSD is prevalent in reptiles and has also been observed in other taxa [10, 23, 31].

During this critical developmental window, slight temperature variations influence enzyme activity and gene expression, leading to differentiation into male or female go-

nads. Specific temperature thresholds vary by species, resulting in three distinct types of TSD [25]:

1. Male-biased TSD – Higher temperatures produce males, while lower temperatures produce females (e.g. crocodilians).
2. Female-biased TSD – Higher temperatures favor females, while lower temperatures favor males (e.g. marine turtles).
3. Mixed TSD – Intermediate temperatures produce males, while extreme temperatures yield females.

Typical temperature ranges for TSD in reptiles include the following:

– Green sea turtles: Mostly males below 28°C, predominantly females above 30°C [42].
– American alligator (Alligator mississippiensis): Males develop around 33°C, while cooler or warmer temperatures favor females [41, 42].
– Painted turtles (Chrysemys picta): Males emerge at intermediate temperatures (27-29°C), while extreme temperatures favor females [41].

For these species, incubation temperature during a specific developmental period determines sex, and minor temperature fluctuations can drastically alter sex ratios [8, 42].

Rising global temperatures pose a serious threat to reptiles with TSD, as skewed sex ratios could affect population stability and long-term survival [14,18,35,37]. A 2020 study by Blechschmidt [6] highlighted the potential extinction risks for green sea turtles due to climate change. This concern extends beyond contemporary reptiles – STD-induced changes in sex ratio have even been speculated as a factor in dinosaur extinction [28, 30].

Green sea turtles exhibit polygynandrous mating behavior, where both males and females mate with multiple partners during the breeding season [22, 34, 36, 43].

Due to this reproductive structure, traditional pair-formation models used in two-sex population dynamics are not applicable. Instead, we employ dynamical models structured by sex to capture population interactions [4, 21].

In our previous work [19,40], we developed sex-structured models to investigate population persistence and extinction risks. This paper extends the framework by incorporating environmental constraints, such as Allee's effects, to explore the interplay between thermal and ecological factors in shaping population dynamics.

In the following section, we present our mathematical model, integrating environmental and thermal constraints into the existing sex-structured framework.

2 Model equations

Mathematical models addressing temperature-dependent sex determination often fall within the broader category of life history models. There are both direct and indirect approaches to incorporating temperature effects. A representative indirect approach was

developed by Murray [30], who modeled spatially distributed nesting regions, each characterized by distinct incubation temperatures. In contrast, our previous work [19, 40] adopted a direct approach by explicitly including the incubation temperature as a parameter in the model.

In this study, we develop a sex-structured and stage-structured dynamical model to describe the population dynamics of green sea turtles. Building on the framework established in our earlier studies, the updated model further incorporates strong Allee effects, introducing nonlinear feedback that reflects ecological constraints on reproduction and survival.

Biologically, green sea turtles progress through four life stages: egg, hatchling, juvenile, and adult (see Fig. 1). Since sex is determined during the egg stage via TSD, we aggregate the life cycle into two functional stages: the egg stage and the adult stage. The adult stage encompasses all post-hatching phases, including reproductively mature individuals. Each stage is further divided into male and female categories.

Let $A_m(t)$ and $A_f(t)$ denote the male and female adult populations at time t, and let $E_m(t)$ and $E_f(t)$ denote the male and female egg populations. The total adult population is given by $A(t)=A_m(t)+A_f(t)$. The governing system of differential equations is

$$\begin{aligned}
&\frac{dA_m}{dt}=\alpha_m E_m-\mu_a A_m,\\
&\frac{dA_f}{dt}=\alpha_f E_f-\mu_a A_f,\\
&\frac{dE_m}{dt}=-\alpha_m E_m+phr_e\left(\frac{A}{C}-1\right)\left(1-\frac{A}{K}\right)fA_m-\mu_e E_m,\\
&\frac{dE_f}{dt}=-\alpha_f E_f+(1-p)hr_e\left(\frac{A}{C}-1\right)\left(1-\frac{A}{K}\right)fA_m-\mu_e E_f,\\
&A_m(0)=A_m^0>0,\quad A_f(0)=A_f^0>0,\quad E_m(0)=E_m^0>0,\quad E_f(0)=E_f^0>0.
\end{aligned}\tag{2.1}$$

The parameter p represents the proportion of eggs that develop into males and is modeled as a function of the mean incubation temperature T. Based on empirical studies, Girondot [16] proposed the following logistic-type function to describe temperature-dependent sex determination in reptiles:

$$p(T)=\frac{1}{1+e^{-(\beta-T)/s}},$$

where β is the pivotal temperature at which the sex ratio is balanced ($p=0.5$), and s is a shape parameter controlling the steepness of the transition. This empirical formulation captures the biological mechanism of TSD, where warmer temperatures favor female development and cooler temperatures favor male development. The adoption of Girondot's empirical function $p(T)$ allows incubation temperature T to enter the model explicitly, linking thermal conditions to sex ratio dynamics.

All parameters in system (2.1) are defined with biologically meaningful units. The maturation rates α_m and α_f, and the mortality rates μ_a and μ_e, are measured in inverse

years, reflecting the rate at which individuals transition between life stages or die. The fundamental model parameter f denotes the average number of female mating partners per male per year and also carries units of inverse years. The quantity r_e represents the average number of eggs laid per female per nesting event and is interpreted as a count of eggs. The hatching success rate h and the sex ratio parameter p are dimensionless proportions. The parameters K and C, representing the carrying capacity and critical mass respectively, are dimensionless in the equations but semantically correspond to population sizes, measured in number of individuals. The nonlinear term $(A/C-1)(1-A/K)$ captures the Allee effect, modeling reduced reproductive success at low population densities and saturation effects at high densities [1, 2, 4]. This formulation allows the model to reflect both ecological vulnerability and demographic thresholds, which are critical for understanding population persistence under environmental and thermal stress.

For notational simplicity, we define a composite parameter $r=r_ehf$, representing the number of hatched eggs per unit of time sired by a single male turtle. Since the individual components r_e, h, and f are readily estimated, we retain their decomposition for interpretability. A detailed description and estimation of all model parameters is provided in Table 1.

Table 1: Estimated parameters for green sea turtle population dynamics.

Parameter	Description	Estimated value	Reference
μ_a	Mortality rate of adult	$1/70$	Implied from [26]
r_e	Average # of eggs per encounter	110	[33]
μ_e	Mortality rate of eggs	$365/45\approx 8.11$	Implied from [26]
α_m	Maturity rate of male eggs	0.001	Implied from [12]
α_f	Maturity rate of female eggs	0.001	Implied from [12]
f	Sexually-encounter rate per male	4	Estimated
p	Proportion of eggs becoming male	Varies	N/A
$1-p$	Proportion of eggs becoming female	Varies	N/A
h	Egg hatching rate	0.25	[39]
C	Allee-critical mass	N/A	N/A
K	Carrying capacity	N/A	N/A
c	Ecological viability ratio	$0<c<1$	N/A
β	Pivotal temperature	$29.34^\circ C$	[16]
s	Shape of transition	1.01	[16]

3 Equilibrium analysis

3.1 Extreme situations

We first consider the simplest dynamics for model (2.1). When $p=0$ or $p=1$, our model predicts population extinction. For instance, when $p=0$, we derive

$$\frac{dE_m}{dt}=-\alpha_m E_m-\mu_e E_m,$$

which implies that $E_m\to 0$ as $t\to\infty$. Consequently, it follows that $A_m\to 0$ as $t\to\infty$. Similarly, since $A_m\to 0$, we obtain $E_f\to 0$ as $t\to\infty$, leading to

$$\frac{dA_f}{dt}=\alpha_f E_f-\mu_a A_f.$$

Since $E_f\to 0$, we conclude that $A_f\to 0$ as $t\to\infty$, confirming population extinction. The case of $p=1$ follows an identical argument, starting from the equation of dE_f/dt.

In the remainder of this paper, we focus exclusively on the biologically relevant case where $0<p<1$.

3.2 Nondimentionalization

We scale the adult population by the Allee critical density C, so that both

$$x_1=\frac{A_m}{C},\quad x_2=\frac{A_f}{C}$$

are dimensionless. The egg populations E_m and E_f are scaled by

$$E_m=\frac{prC}{\mu_e+\alpha_f}y_1,\quad E_f=\frac{(1-p)rC}{\mu_e+\alpha_f}y_2$$

so that y_1 and y_2 have no dimension. We choose the expected lifespan of the adult population, $1/\mu_a$, to scale the time $\tau=t/(1/\mu_a)=\mu_a t$. Denote C/K by $c, c=C/K<1$ measure the critic density by the carrying capacity. Then the dimensionless version of the system (2.1) is

$$\frac{dx_1}{d\tau}=\frac{\alpha_m pr}{\mu_a(\mu_e+\alpha_f)}y_1-x_1, \tag{3.1a}$$

$$\frac{dx_2}{d\tau}=\frac{\alpha_m(1-p)r}{\mu_a(\mu_e+\alpha_f)}y_2-x_2, \tag{3.1b}$$

$$\frac{dy_1}{d\tau}=\frac{\mu_e+\alpha_f}{\mu_a}\left(-y_1\frac{\alpha_m+\mu_e}{\mu_e+\alpha_f}+\big((x_1+x_2)-1\big)\big(1-c(x_1+x_2)\big)x_1\right), \tag{3.1c}$$

$$\frac{dy_2}{d\tau}=\frac{\mu_e+\alpha_f}{\mu_a}\big(-y_2+\big((x_1+x_2)-1\big)\big(1-c(x_1+x_2)\big)x_1\big). \tag{3.1d}$$

The following biological meaningful re-parameterizations are introduced early to facilitate our mathematical management:

$$R_0^m=\frac{\alpha_m pr}{\mu_a(\alpha_m+\mu_e)},$$

$$
\begin{aligned}
R_0^f &= \frac{\alpha_f(1-p)r}{\mu_a(\alpha_f+\mu_e)},\\
Q &= \frac{R_0^f}{R_0^m} = \frac{(1-p\alpha_f)/(\alpha_f+\mu_e)}{p\alpha_m/(\alpha_m+\mu_e)},\\
R_c &= R_0^m\frac{(1-c)^2}{4c} = \frac{\alpha_m pr}{\mu_a(\alpha_m+\mu_e)}\frac{(1-c)^2}{4c}.
\end{aligned}
\tag{3.2}
$$

3.3 Persistent equilibrium and population viability

The existence of equilibria in system (3.1) is mathematically manageable. The Eqs. (3.1c)-(3.1d) yield the following expressions:

$$
\begin{aligned}
y_1 &= \frac{\mu_e+\alpha_f}{\alpha_m+\mu_e}\big((x_1+x_2)-1\big)\big(1-c(x_1+x_2)\big)x_1 \triangleq \phi_1(x_1,x_2),\\
y_2 &= \big((x_1+x_2)-1\big)\big(1-c(x_1+x_2)\big)x_1 \triangleq \phi_2(x_1,x_2).
\end{aligned}
\tag{3.3}
$$

Substituting them into the first two equations, we arrive at the following:

$$
\begin{aligned}
R_0^m(x_1+x_2-1)\big(1-c(x_1+x_2)\big)x_1 - x_1 &= 0,\\
R_0^f(x_1+x_2-1)\big(1-c(x_1+x_2)\big)x_1 - x_2 &= 0.
\end{aligned}
\tag{3.4}
$$

From the above, it follows that at equilibrium we have $x_2 = Qx_1$. This reduces the computations for determining the equilibrium to a single equation for x_1 alone

$$
R_0^m x_1\big((1+Q)x_1-1\big)\big(1-c(1+Q)x_1\big) - x_1 = 0. \tag{3.5}
$$

The trivial equilibrium $x_1 = 0$ satisfies (3.5), which implies that $E^0 = (0,0,0,0)$ is always an equilibrium. This represents the population collapse, so we refer to E^0 as the collapsed equilibrium.

Theorem 3.1. *The system* (3.1) *unconditionally admits the collapsed equilibrium* $E^0 = (0,0,0,0)$.

Non-trivial equilibria are obtained by solving the quadratic equation

$$
\big((1+Q)x_1-1\big)\big(1-c(1+Q)x_1\big) - 1/R_0^m = 0. \tag{3.6}
$$

For the quadratic equation (3.6):

– If $R_c < 1$, there is no real solution.

– If $R_c > 1$, two positive equilibria x_1^+ and x_1^- emerge, given by

$$
\begin{aligned}
x_1^+ &= \frac{1+c+\sqrt{1-\big(1+R_0^m\big)/R_c}}{2c(1+Q)},\\
x_1^- &= \frac{1+c-\sqrt{1-\big(1+R_0^m\big)/R_c}}{2c(1+Q)}.
\end{aligned}
\tag{3.7}
$$

– When $R_c=1$, the solutions are x_1^+ and x_1^- coalesce, resulting in a saddle-node bifurcation of equilibrium.

By substituting $x_1^+, x_2^+ = Qx_1^+$, and similarly $x_1^-, x_2^- = Qx_1^-$ into (3.3), we finally obtain

$$y_i^+ = \phi_i(x_1^+, x_2^+), \quad y_i^- = \phi_i(x_1^-, x_2^-), \quad i=1,2.$$

These algebraic calculations confirm that the system (3.1) exhibits a saddle-node bifurcation at $R_c=1$, thus establishing the existence of persistent equilibria.

Theorem 3.2. *Consider the system* (3.1).

– *When $R_c>1$, there are two positive equilibria*

$$E^+ = (x_1^+, x_2^+, y_1^+, y_2^+), \quad E^- = (x_1^-, x_2^-, y_1^-, y_2^-).$$

– *When $R_c=1$, E^+ and E^- coalesce, leading to a saddle-node bifurcation.*

– *When $R_c<1$, there are no persistent equilibria and population collapse occurs.*

A visual representation of Theorem 3.2 is depicted in Fig. 3.

3.4 Local stability of the collapsed equilibrium

The Jacobian matrix of the full system (3.1) evaluated at the collapsed equilibrium $E^0 = (0,0,0,0)$ is given by

$$J = \begin{bmatrix} -1 & 0 & M_1 & 0 \\ 0 & -1 & 0 & M_2 \\ -\delta & -\delta & -\delta M_3 & 0 \\ -\delta & -\delta & 0 & -\delta \end{bmatrix},$$

where

$$M_1 = \frac{\alpha_m p r}{\mu_a(\mu_e+\alpha_f)}, \quad M_2 = \frac{\alpha_m(1-p)r}{\mu_a(\mu_e+\alpha_f)}, \quad M_3 = \frac{\alpha_m+\mu_e}{\mu_e+\alpha_f},$$

and $\delta = 1/\epsilon$. The characteristic equation of J is given by $(1+\lambda)f(\lambda)=0$, where

$$f(\lambda) = \lambda^3 + \big(\delta M_3 + (1+\delta)\big)\lambda^2 + \big(M_1\delta + (M_2+1)\delta + \delta(1+\delta)M_3\big)\lambda + M_1\delta^2 + (M_2+1)\delta^2.$$

It is straightforward to verify that

$$\big(\delta M_3 + (1+\delta)\big)\big(M_1\delta + (M_2+1)\delta + \delta(1+\delta)M_3\big) > M_1\delta^2 + (M_2+1)\delta^2.$$

From the Routh-Hurwitz criterion it follows that all eigenvalues of J have negative real parts. We now state this result formally.

Theorem 3.3. *The collapsed equilibrium E^0 of system* (3.1) (*and the original system* (2.1)) *is always locally asymptotically stable for all parameter values.*

We will subsequently analyze the global stability of the collapsed equilibrium using a singular perturbation approach.

4 A singular perturbation approach

The significant difference in time scales between the adult turtle population and the egg population allows us to reduce the original four-dimensional nonlinear model (2.1) to a lower-dimensional system using a singular perturbation approach. Specifically, the incubation period of eggs, given by $1/(\mu_e+\alpha_f)$, is approximately 40-45 days, whereas the average lifespan of an adult turtle, $1/\mu_a$, is around 70 years. This substantial disparity implies that the ratio $\mu_a/(\mu_e+\alpha_f)$ can be treated as a small parameter.

Introducing the small parameter $\epsilon=\mu_a/(\mu_e+\alpha_f)$, we rescale the time variable and rewrite the system (3.1) in the following dimensionless form:

$$\begin{aligned}
\frac{dx_1}{d\tau}&=\frac{\alpha_m pr}{\mu_a(\mu_e+\alpha_f)}y_1-x_1,\\
\frac{dx_2}{d\tau}&=\frac{\alpha_m(1-p)r}{\mu_a(\mu_e+\alpha_f)}y_2-x_2,\\
\epsilon\frac{dy_1}{d\tau}&=-y_1\frac{\alpha_m+\mu_e}{\mu_e+\alpha_f}+\big((x_1+x_2)-1\big)\big(1-c(x_1+x_2)\big)x_1,\\
\epsilon\frac{dy_2}{d\tau}&=-y_2+\big((x_1+x_2)-1\big)\big(1-c(x_1+x_2)\big)x_1.
\end{aligned}\tag{4.1}$$

System (4.1) is in the standard form of a singular perturbation problem. In this formulation, y_1 and y_2 are referred to as fast variables, while x_1 and x_2 are slow variables.

4.1 Dynamics on the slow manifold

To derive the quasi-steady states, we set $\epsilon=0$ in the equations for the fast variables. Substituting the resulting expressions for y_1 and y_2 (from (3.3)) into the equations for the slow variables yields the following reduced two-dimensional system:

$$\begin{aligned}
\frac{dx_1}{d\tau}&=R_0^m(x_1+x_2-1)\big(1-c(x_1+x_2)\big)x_1-x_1,\\
\frac{dx_2}{d\tau}&=R_0^f(x_1+x_2-1)\big(1-c(x_1+x_2)\big)x_1-x_2.
\end{aligned}\tag{4.2}$$

An insightful property of (4.2) is obtained by considering

$$\frac{d}{d\tau}\big(R_0^f x_1-R_0^m x_2\big)=-R_0^f x_1+R_0^m x_2=-\big(R_0^f x_1-R_0^m x_2\big),$$

which integrates to

$$R_0^f x_1-R_0^m x_2=\big(R_0^f x_1(0)-R_0^m x_2(0)\big)e^{-\tau}\ \longrightarrow\ 0\quad\text{as}\quad\tau\ \to\ \infty.$$

Hence, the line $R_0^f x_1-R_0^m x_2=0$ is globally attracting. In the long term, the trajectories of (4.2) satisfy $R_0^f x_1=R_0^m x_2$.

Substituting $x_2 = Qx_1$ with $Q = R_0^f / R_0^m$ in (4.2) reduces the dynamics to a single equation for x_1

$$\frac{dx_1}{d\tau} = R_0^m x_1 \big((1+Q)x_1 - 1\big)\big(1 - c(1+Q)x_1\big) - x_1. \tag{4.3}$$

One verifies by routine calculation that $x_1 = 0$ is a locally asymptotically stable equilibrium, corresponding to the collapsed equilibrium E^0. Nonzero equilibria of (4.3) arise from the quadratic condition (3.6). Specifically,

- If $R_c < 1$, the only equilibrium is $x_1 = 0$ (extinction).
- If $R_c > 1$, there exist two positive equilibria x_1^- and x_1^+ given by (3.7).

Rewrite (4.3) as

$$\frac{dx_1}{d\tau} = -R_0^m c(1+Q)^2 x_1 (x_1 - x_1^-)(x_1 - x_1^+),$$

which reveals that, when $R_c > 1$, the equilibria at $x_1 = 0$ and $x_1 = x_1^+$ are asymptotically stable, while $x_1 = x_1^-$ is unstable. Moreover, if $R_c < 1$, the extinction equilibrium $x_1 = 0$ is globally asymptotically stable.

Because $R_0^f x_1 - R_0^m x_2 \to 0$, the long-term behavior of the slow system (4.2) is summarized in the following result.

Theorem 4.1. *Consider the slow dynamics governed by system* (4.2).

- *The extinction equilibrium* $(0,0)$ *is always locally asymptotically stable and globally asymptotically stable if* $R_c < 1$.
- *If* $R_c > 1$, *two nontrivial equilibria exist:* (x_1^+, Qx_1^+) *and* (x_1^-, Qx_1^-).
- *For* $R_c > 1$, *the equilibrium* (x_1^-, Qx_1^-) *is unstable, while* (x_1^+, Qx_1^+) *is locally asymptotically stable.*

The second part of Theorem 4.1 demonstrates the bistable nature of the system when $R_c > 1$. Figs. 5 and 6 illustrate these dynamics. The case of $R_c < 1$ is shown in Fig. 4.

4.2 Global stability of the collapsed equilibrium

If $\epsilon \ll 1$, we further study the global stability of the collapsed equilibrium E^0 of the four-dimensional system (3.1).

Theorem 4.2. *Consider the full system* (3.1) *with* $\epsilon \ll 1$. *If* $R_c < 1$, *the collapsed equilibrium* E^0 *is globally asymptotically stable.*

The proof of Theorem 4.2 is carried out applying a theorem from an early work by Hoppensteadt [20].

We now re-state Hoppensteadt's theorem. Let $x\in\mathbb{R}^n$ and $y\in\mathbb{R}^m$. Consider a general perturbation problem

$$\begin{aligned}\frac{dx}{dt}&=f(x,y,\epsilon),\\ \epsilon\frac{dy}{dt}&=g(x,y,\epsilon),\end{aligned}\tag{4.4}$$

where ϵ is a small positive parameter. Consequently, x and y are called slow variables and fast variables. Let $y=\phi(x)$ be the implicit function defined by $g(x,y,0)=0$. Then a reduced system of the full system (4.4) is the following:

$$\frac{dx}{dt}=f\big(x,\phi(x),0\big).\tag{4.5}$$

Let (x^*,y^*) be an equilibrium of the system (4.5), that is, $g(x^*,y^*,0)=0$ and $f(x^*,y^*),0)=0$, then Theorem 4.3 (below), a special case of Hoppensteadt's theorem [20, Theorem 2], helps characterize the dynamics of this system near the slow manifold.

Theorem 4.3. *Assume*

(i) The slow manifold, $g(x,y,0)=0$, is a graph, that is, there exists a function $y=\phi(x)$ such that $g(x,\phi(x),0)\equiv 0$.

(ii) Both $f(x,y,\epsilon)$ and $g(x,y,\epsilon)$ have continuous and bounded derivatives with respect to ϵ and the state variables x and y.

(iii) The system $dx/dt=f(x,\phi(x),0)$ has a globally stable fixed point x^* and $y^*=\phi(x^*)$. The matrix $(f_x-f_yg_y^{-1}g_x)(x^*,y^*,0)$ has all eigenvalues with negative real parts.

(iv) The zero solution of the system $dY/d\tau=g(\xi,\phi(\xi)+Y,0)$ is globally stable for any ξ.

(v) The eigenvalues of matrix $g_y(x^*,y^*,0)$.

Then if there is a locally asymptotically stable equilibrium of the full system, then it is globally asymptotically stable when ϵ is small.

Now we present a rigorous proof to Theorem 4.2.

Proof. In Hoppensteadt's original notation in [20], if we let $(\tilde{x}(t,\epsilon),\tilde{y}(t,\epsilon))$ denote the equilibrium solution (x_0,y_0) of the full system, D be R^m and $E_\xi=R^n$, then Theorem 4.2 follows as a special case. Consequently, we only have to verify that all 5 hypothesis are satisfied for the full system (3.1).

In our model f and g are

$$f=\begin{bmatrix}f_1\\ f_2\end{bmatrix}=\begin{bmatrix}\dfrac{\alpha_m pr}{\mu_a(\mu_e+\alpha_f)}y_1-x_1\\ \dfrac{\alpha_m(1-p)r}{\mu_a(\mu_e+\alpha_f)}y_2-x_2\end{bmatrix},$$

$$g=\begin{bmatrix} g_1 \\ g_2 \end{bmatrix}=\begin{bmatrix} c-y_1\dfrac{\alpha_m+\mu_e}{\mu_e+\alpha_f}+\big((x_1+x_2)-1\big)\big(1-c(x_1+x_2)\big)x_1 \\ -y_2+\big((x_1+x_2)-1\big)\big(1-c(x_1+x_2)\big)x_1 \end{bmatrix}.$$

Note: In our case, both f and g are independent of the small parameter ϵ.

(i) The slow manifold is the graph given by (3.3) $M_0: y=\phi(x), y\in R^2$ and $x\in R^2$,

$$\begin{aligned} y_1&=\phi_1(x_1,x_2)=\frac{\mu_e+\alpha_f}{\alpha_m+\mu_e}\big((x_1+x_2)-1\big)\big(1-c(x_1+x_2)\big)x_1, \\ y_2&=\phi_2(x_1,x_2)=\big((x_1+x_2)-1\big)\big(1-c(x_1+x_2)\big)x_1. \end{aligned}$$

(ii) The continuity and boundedness of the derivative of f and g are obvious.

(iii) The eigenvalues of matrix $(f_x-f_yg_y^{-1}g_x)(0,0,0,0)$. Here are f_x, f_y, g_x and g_y at $(0,0,0,0)$:

$$f_x=\begin{bmatrix} -1 & 0 \\ 0 & -1 \end{bmatrix},\quad f_y=\begin{bmatrix} M_1 & 0 \\ 0 & M_2 \end{bmatrix},\quad g_x=\begin{bmatrix} -1 & 0 \\ 0 & -1 \end{bmatrix},\quad g_y=\begin{bmatrix} -M_3 & 0 \\ 0 & -1 \end{bmatrix}.$$

Thus,

$$J=\big(f_x-f_yg_y^{-1}g_x\big)(0,0,0,0)=\begin{bmatrix} -1-\dfrac{M_3}{M_1} & 0 \\ 0 & -1-\dfrac{1}{M_2} \end{bmatrix}$$

has two negative eigenvalues. Theorem 3.3 ensures that $(0,0)$ is a globally stable equilibrium for the system $dx/d\tau=f(x,\phi(x))$.

(iv)

$$\frac{dY}{d\tau}=g\big(\xi,\phi(\xi)+Y\big)=\begin{bmatrix} -M_3 & 0 \\ 0 & -1 \end{bmatrix}\begin{bmatrix} y_1 \\ y_2 \end{bmatrix}$$

is a linear system that is independent of the parameter ξ. The zero solution of the above system is globally asymptotically stable for any ξ, because all eigenvalues are negative.

(v) Since $g_y(0,0)$ has eigenvalues $\lambda=-M_3$ and $\lambda=-1$, the item (v) of the hypothesis is validated.

This completes the verification and the proof of Theorem 4.2. □

5 Reparameterization and parameter estimation

In the preceding sections, we introduced dimensionless quantities c, R_0^m, R_0^f, R_c, and Q to simplify the mathematical analysis. In the following, we provide their biological and ecological interpretations.

5.1 Ecological viability ratio: $c = C/K$

Here, C denotes the critical population density (or Allee threshold) below which growth is impeded by factors such as mate limitation, loss of cooperative behaviors or reduced genetic diversity [11]. The parameter K is the carrying capacity, that is, the maximum population size that is sustainable by the available resources. Thus, the ratio $c = C/K$ measures the proportion of carrying capacity required to maintain the population under environmental pressures.

5.2 Basic reproductive number for males: R_0^m

We decompose R_0^m as

$$R_0^m = \frac{1}{\mu_a} \frac{\alpha_m}{\alpha_m + \mu_e} phr_e f. \tag{5.1}$$

Each factor represents a key stage in male turtle reproduction:

- $1/\mu_a$ is the average lifespan of an adult male.
- $\alpha_m/(\alpha_m+\mu_e)$ is the probability that a male hatchling survives to adulthood.
- f is the average number of mating encounters per male per unit of time.
- r_e is the number of eggs laid per mated female, each hatching with probability h.
- p is the probability that a hatchling is male, reflecting temperature-dependent sex determination.

Consequently, R_0^m gives the expected number of male offspring produced by a single male during its lifetime, serving as a key metric for male population viability.

5.3 Allee-adjusted reproductive number: R_c

Our analysis shows that the population's persistence hinges on the Allee-adjusted reproductive number

$$R_c = R_0^m \frac{(1-c)^2}{4c}.$$

The term $(1-c)^2/(4c)$ modulates R_0^m by accounting for population constraints, reflecting how environmental conditions regulate reproductive success. Defining the environmental viability constraint as

$$\mathrm{Env} = \frac{4c}{(1-c)^2},$$

the condition for long-term persistence is

$$R_0^m > \mathrm{Env}.$$

If $c \ll 1$, the Allee effect is weak and this condition is easily met. In contrast, when $c \approx 1$, environmental restrictions are severe and achieving $R_0^m > \mathrm{Env}$ becomes more difficult.

5.4 Adult sex ratio: Q

The parameter

$$Q=\frac{R_0^f}{R_0^m}=\frac{(1-p)\alpha_f/(\alpha_f+\mu_e)}{p\alpha_m/(\alpha_m+\mu_e)}$$

compares the female and male basic reproductive numbers. Here,

$$s_f=\frac{(1-p)\alpha_f}{\alpha_f+\mu_e},\quad s_m=\frac{p\alpha_m}{\alpha_m+\mu_e}$$

are the probabilities that a female or male hatchling, respectively, survives to adulthood. Hence,

$$Q=\frac{s_f}{s_m}=\lim_{\tau\to\infty}\frac{x_2}{x_1}=\lim_{t\to\infty}\frac{A_f}{A_m}$$

determines the long-term adult sex ratio of females to males. This ratio remains fixed at Q regardless of whether the population persists or goes extinct.

5.5 Parameter estimations

The life history of sea turtles is well documented in research articles, and several open-access sources provide reliable estimates of key biological parameters. For example, sea turtles lay an average of 110 eggs per nest, as reported in [13, 33]. The hatchling survival rates, estimated as $a_m=a_f=0.001$, can be found in [12, 13]. A relevant excerpt from [12] states:

> "Only about one in 1,000 turtles survives to adulthood. Hatchlings die of dehydration if they do not reach the ocean quickly enough. Birds, crabs, and other predators also prey on young turtles".

The hatching success rate of eggs is $h=25\%$, as reported in [39]. Table 1 summarizes the estimated values and references for the model parameters.

It is important to note that parameter estimates may vary across different green sea turtle populations, and values reported in the literature may differ due to regional ecological factors and methodological variations.

6 Results

In executing our model, we treat the ecological viability ratio c and the probability p as independent parameters, varying within the interval $(0,1)$. All other parameter values are taken from Table 1.

6.1 The interplay between incubation temperature T and ecological viability ratio c

The parameter p represents the proportion of eggs that develop into males, which is determined by the mean incubation temperature of nests (T). Applying maximum likelihood estimation to a logistic-like function, Girondot [16] proposed the following relationship:

$$p(T)=\frac{1}{1+e^{-(\beta-T)/s}}. \tag{6.1}$$

Substituting $p(T)$ into the expression for R_c in (3.2), we obtain the reparameterized form

$$R_c(T,c)=\frac{1}{1+e^{-(\beta-T)/s}}\,\frac{rm\alpha_m}{\mu_a(\alpha_m+\mu_e)}\,\frac{(1-c)^2}{4c}. \tag{6.2}$$

The contour curve of $R_c(T,c)=1$ on the (T,c)-plane is depicted in Fig. 2. The upper region corresponds to population collapse, while the lower region predicts population persistence.

As the mean incubation temperature increases, the persistence region shrinks rapidly, indicating that even moderate environmental conditions (that is, midrange values of c) cannot prevent the collapse of the population. For instance, if $c=0.05$, the model predicts that population collapse occurs at an incubation temperature of $T=30.1847^\circ$C.

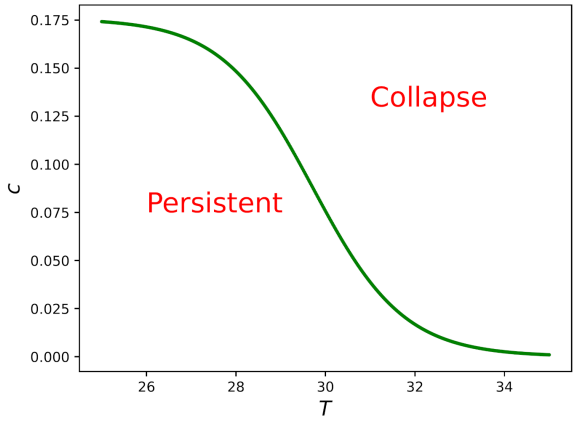

Figure 2: The combined impact of incubation temperature (T) and ecological viability ratio (c) on the persistence of the green sea turtle population. On the (T,c)-plane, the green curve delineates the boundary between population collapse and persistence.

6.2 Catastrophic collapse

Our model predicts that population collapse can occur abruptly, as illustrated in Fig. 2. However, population extinction does not occur in a continuous fashion. Instead, it follows a hysteretic trajectory, where the population may persist despite adverse conditions until crossing a critical threshold, after which a sudden collapse occurs.

The catastrophic collapse emerges when the parameters c and T cross the boundary corresponding to the saddle-node bifurcation. Initially, when $R_c > 1$, the population remains stable at x_1^+ – the larger equilibrium in the left panel of Fig. 3. As c and T vary, e.g. keeping c fixed while increasing T the equilibrium x_1^+ gradually shifts towards x_1^-, leading to a continuous decline in population size.

However, as soon as c and T cross the bifurcation threshold, the equilibria x_1^+ and x_1^- vanish, forcing the population to collapse to the extinct equilibrium. This sudden transition results in a catastrophic population decline.

For the case where $R_c < 1$, Fig. 4 presents time series trajectories for a wide range of initial conditions, illustrating the collapse of the green sea turtle population.

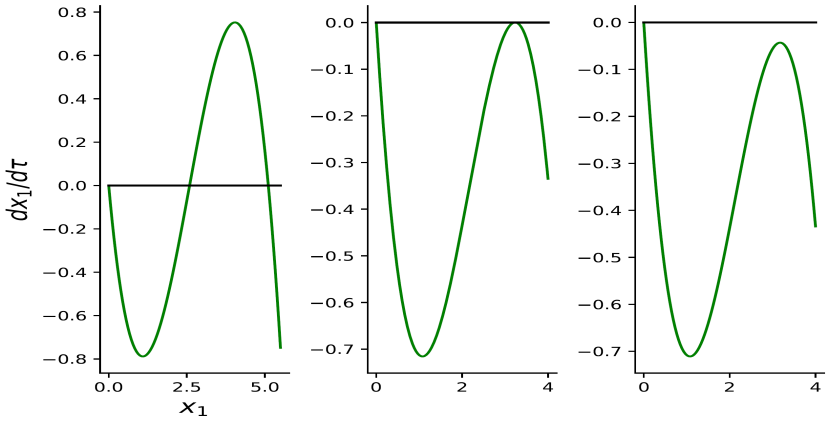

Figure 3: A hysteretic demonstration of population collapse. The left, middle, and right panels correspond to cases where $R_c > 1, R_c = 1$, and $R_c < 1$, respectively. The left panel shows population persistence, whereas the middle and right panels depict the transition to population collapse.

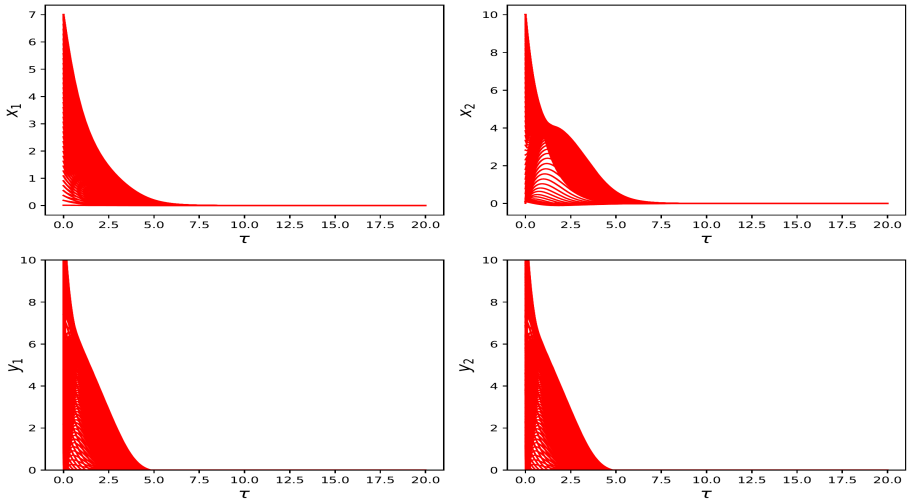

Figure 4: Population collapse is confirmed when $R_c < 1$ for a large set of initial conditions.

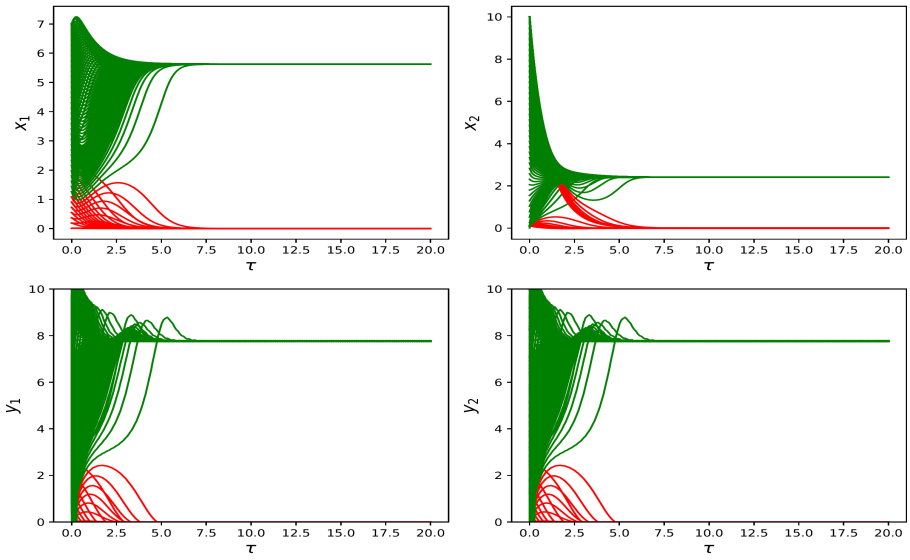

Figure 5: For $R_c > 1$, the full model (3.1) exhibits bi-stable equilibrium dynamics. Red trajectories approach the collapsed equilibrium E^0, while green trajectories approach the persistent equilibrium E^+.

6.3 Bi-stable dynamics

Theoretically, the emergence of bi-stability in equilibria is an intriguing phenomenon. However, when applying the model to an existing green sea turtle population under the assumption that $R_c > 1$, extinction does not occur, as the initial conditions remain outside the attraction domain of the collapsed equilibrium E^0.

A phase portrait and its corresponding time series plots are shown in Fig. 6 for the slow variables in model (3.4).

7 Discussion and conclusion

Using a sex-structured and age-structured dynamical model grounded in the life history of green sea turtles, we demonstrate how environmental and thermal constraints shape their population dynamics. The Allee-adjusted reproductive number serves as a threshold criterion for extinction, capturing the interplay between demographic vulnerability and ecological stress. Our model results highlight the serious risk of extinction facing green sea turtles, and predict that if extinction occurs, it will manifest as a catastrophic collapse rather than a gradual decline.

We emphasize the interplay between climate change and environmental deterioration. Global warming is a real and pressing issue, placing the future of green sea turtles at serious risk. In addition to rising temperatures, the degradation of environmental conditions, quantified by the ecological viability ratio c, further threatens population persistence.

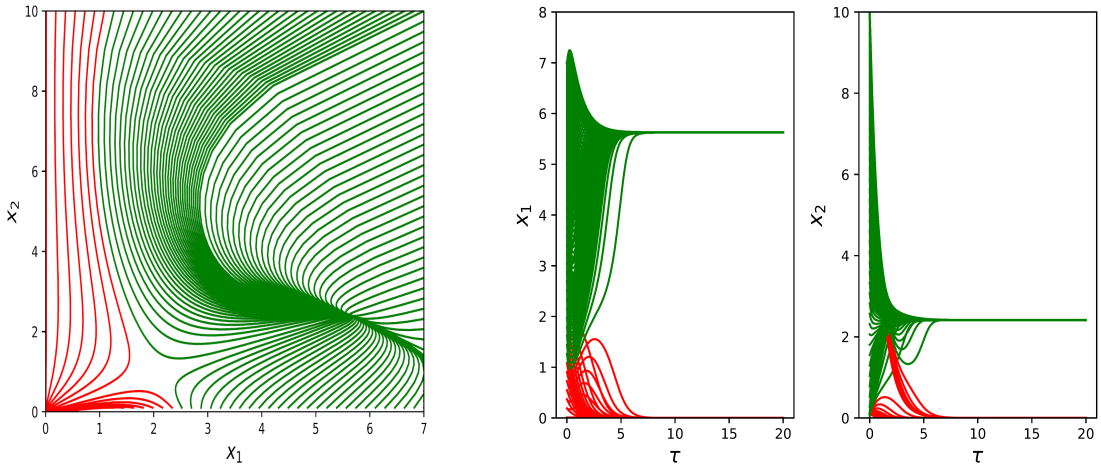

Figure 6: Bi-stability of the slow variables. The left panel presents a phase portrait, while the right panel depicts the corresponding time series trajectories.

Coastal development, human activities, sea level rise, and increased storm events directly impact nesting beaches and food availability for green sea turtles, causing ecological stress. Plastic pollution, which contaminates both nesting beaches and marine habitats [23], has a direct effect on R_c. Climate change not only skews the sex ratio, pushing populations toward collapse, but also intensifies storm activity, leading to nest flooding and higher hatchling mortality rates.

From an evolutionary biology perspective, one might hope that climate change and rising temperatures occur gradually, allowing organisms the necessary time to adapt. A natural question arises: Can the evolutionary response of the green sea turtle mitigate these threats?

Recent findings by Rickwood *et al.* [35] provide hope in this regard. Their study suggests that climate change and rising temperatures are already altering the life history of green sea turtles. Specifically, green turtles are adjusting their nesting timing in response to temperature shifts:

> "Green turtles are adjusting their nesting timing in response to climate change, advancing by approximately 6.47 days for every 1°C increase in sea temperature" [35].

Our mathematical approach to the sex-structured and stage-structured dynamical model is built on the discrepancy in time scales, analyzed through singular perturbation methods. The global attraction of the collapsed equilibrium E^0 is mathematically rigorous and provides a key criterion for population extinction. However, we have not explored the stability of the persistent equilibrium for the full system (3.1), although its behavior was fully characterized for the reduced system (3.4). This leaves an open question for future research.

A potential future direction would be to investigate the correlation between critical mass C, carrying capacity K, and mean incubation temperature T, further refining our understanding of population persistence under changing environmental conditions.

This study highlights the combined influence of thermal conditions and environmental constraints on the dynamics of the green sea turtle population, where TSD plays a critical role in their life history. We believe that the sex-structured and stage-structured modeling framework, which incorporates strong Allee effects, can be extended to other reptile species exhibiting TSD, providing broader ecological insights.

References

[1] W. C. Allee, *Animal aggregations*, Q. Rev. Biol., 2:367–398, 1927.

[2] W. C. Allee, *Animal Aggregations: A Study in General Sociology*, University of Chicago Press, 1931.

[3] V. K. Beckwith and M. M. P. B. Fuentes, *Microplastic at nesting grounds used by the northern gulf of Mexico loggerhead recovery unit*, Mar. Pollut. Bull., 131:32–37, 2018.

[4] L. Berec, *Mate search and mate-finding Allee effect: On modeling mating in sex-structured population models*, Theor. Ecol., 11:225–244, 2018.

[5] K. Bjorndal and G. Zug, *Growth and age of sea turtles*, in: Biology and Conservation of Sea Turtles, Smithsonian Institution Press, 599–600, 1995.

[6] J. Blechschmidt, M. Wittmann, and C. Blüml, *Climate change and green sea turtle sex ratio-preventing possible extinction*, Genes, 11:588, 2020.

[7] J. J. Bull, *Evolution of Sex Determining Mechanisms*, Benjamin/Cummings, 1983.

[8] J. J. Bull, *Sex determination in reptiles*, Q. Rev. Biol., 55:3–21, 1983.

[9] M. Charnier, *Action de la température sur la sex-ratio chez l'embryon d'Agama agama (Agamidae: Lacertilien)*, C. R. Séances Soc. Biol. Fil., 160:620–622, 1966.

[10] A. Cree, M. B. Thompson, and C. H. Daugherty, *Tuatara sex determination*, Nature, 375:543–543, 1995.

[11] J. M. Drake and A. M. Kramer, *Allee effects*, Nature Education Knowledge, 3(10):2, 2011.

[12] Florida Fish and Wildlife Conservation Commission, *Sea Turtle FAQ*. `https://myfwc.com/research/wildlife/sea-turtles/florida/faq/`

[13] L. E. Fowler, *Hatching success and nest predation in the green sea turtle, Chelonia mydas, at Tortuguero, Costa Rica*, Ecology, 60:946–955, 1979.

[14] M. Fuentes, C. Limpus, and M. Hamann, *Vulnerability of sea turtle nesting grounds to climate change*, Glob. Change Biol., 17:140–153, 2011.

[15] G. Gerosa et al., *Sea Turtle Handling Guidebook for Fishermen – Teaching Book*, RAC/SPA Tunis, 2001.

[16] M. Girondot, *Statistical description of temperature-dependent sex determination using maximum likelihood*, Evol. Ecol. Res., 1:479–486, 1999.

[17] J. M. Hall, *Temperature-dependent sex determination in reptiles*, Herp Magazine, 2021. `https://herpetoculturenetwork.com/temperature-dependent-sex-determination-in-reptiles/`

[18] G. C. Hays, A. C. Broderick, F. Glen, and B. J. Godley, *Climate change and sea turtles: A 150-year reconstruction of incubation temperatures at a major marine turtle rookery*, Glob. Change Biol., 9:642–646, 2003.

[19] C. Herrera, E. Guerra, V. Penalver, A. Rosas, Y. Wei, J. Pringle, B. Espinoza, and B. Song, *The impact of temperature-dependent sex determination on the population dynamics of green sea turtles (Chelonia mydas)*, Bionatura, 5:1029–1038, 2020.
[20] F. Hoppensteadt, *Asymptotic stability in singular perturbation problems. II: Problems having matched asymptotic expansion solutions*, J. Differential Equations, 15:510–521, 1974.
[21] M. Iannelli, M. Martcheva, and F. A. Milner, *Gender-Structured Population Modeling: Mathematical Methods, Numerics, and Simulations*, in: Frontiers in Applied Mathematics, Vol. 31, SIAM, 2005.
[22] J. Lasala, C. Hughes, and J. Wyneken, *Breeding sex ratio and population size of loggerhead turtles from Southwestern Florida*, PLoS ONE, 13(1):e0191615, 2018.
[23] A. Lusher, *Microplastics in the marine environment: Distribution, interactions and effects*, in: Marine Anthropogenic Litter, Springer, 245–307, 2015.
[24] P. Lutz, J. Musick, and J. Wyneken, *The Biology of Sea Turtles, Volume II*, CRC Press, 2002.
[25] A. Martínez-Juárez and N. Moreno-Mendoza, *Mechanisms related to sexual determination by temperature in reptiles*, J. Therm. Biol., 85:102400, 2019.
[26] MassWildlife's Natural Heritage & Endangered Species Program, *Green Sea Turtle: A Species of Greatest Conservation Need in the MA State Wildlife Action Plan*. `https://www.mass.gov/info-details/green-sea-turtle`
[27] Y. Matsumoto and D. Crews, *Molecular mechanisms of temperature-dependent sex determination in the context of ecological developmental biology*, Mol. Cell. Endocrinol., 354:103–110, 2012.
[28] D. Miller, J. Summers, and S. Silber, *Environmental versus genetic sex determination: A possible factor in dinosaur extinction?*, Fertil. Steril., 81:954–964, 2004.
[29] K. T. Moeller, *Temperature-dependent sex determination in reptiles*. `https://embryo.asu.edu/pages/temperature-dependent-sex-determination-reptiles`
[30] J. D. Murray, *Mathematical biology: I. An introduction*, in: Interdisciplinary Applied Mathematics, Vol. 17, Springer-Verlag, 2002.
[31] N. Nelson, A. Cree, M. Thompson, S. Keall, and C. Daugherty, *Temperature-dependent sex determination in tuatara*, in: Temperature-Dependent Sex Determination in Vertebrates, Smithsonian Institution Press, 53–58, 2004.
[32] NOAA, *Green turtle*. `https://www.fisheries.noaa.gov/species/green-turtle`
[33] Olive Ridley Project, *How many eggs does a sea turtle lay?* `https://oliveridleyproject.org/ufaqs/how-many-eggs-does-a-sea-turtle-lay/`
[34] PetShun, *Green sea turtles: Do they mate for life?*, 2024. `https://petshun.com/article/do-green-sea-turtles-mate-for-life`
[35] M. L. Rickwood, E. Tucker, D. Beton, S. Davey, B. J. Godley, R. T. E. Snape, E. Postma, and A. C. Broderick, *Individual plasticity in response to rising sea temperatures contributes to an advancement in green turtle nesting phenology*, Proc. R. Soc. B: Biol. Sci., 292:20241809–20241809, 2025.
[36] Science Daily, *Who's your daddy? Good news for threatened sea turtles*. `https://www.sciencedaily.com/releases/2018/02/180207151834.htm`
[37] P. S. Tomillo et al., *Global analysis of the effect of local climate on the hatchling output of leatherback turtles*, Sci. Rep., 5:16789, 2015.
[38] N. Valenzuela and V. Lance, *Temperature-Dependent Sex Determination in Vertebrates*, Smithsonian Institution Press, 2004.
[39] G. Visconti, G. Scopelliti, F. Caldareri, M. Agate, I. Cambera, A. Sulli, and M. Arculeo, *Hatching success of Caretta caretta on a Mediterranean volcanic beach: Impacts from environmental parameters and substrate composition*, J. Coast. Res., 38:603–612, 2022.

[40] Y. Wei, B. Song, and S. Yuan, *Dynamics of a ratio-dependent population model for green sea turtle with age structure*, J. Theor. Biol., 516:110614, 2021.
[41] P. S. Western, J. L. Harry, J. A. M. Graves, and A. H. Sinclair, *Temperature-dependent sex determination in the American alligator: AMH precedes SOX9 expression*, Dev. Dyn., 216:411–419, 1999.
[42] S. Yamaguchi and Y. Iwasa, *Temperature-dependent sex determination, realized by hormonal dynamics with enzymatic reactions sensitive to ambient temperature*, J. Theor. Biol., 453:146–155, 2018.
[43] M. Ye, H. Chen, M.-Y. Li, J. X. Duan, and P.-P. Li, *Captive green turtles (Chelonia mydas)*, Herpetol. Conserv. Biol., 15(2):284–292, 2020.